applied optics

Reduction of the effects of angle errors for a channeled spectropolarimeter

Xueping Ju,[1,2] Bin Yang,[1,2] Junqiang Zhang,[1,*] and Changxiang Yan[1]

[1]Changchun Institute of Optics, Fine Mechanics and Physics, Chinese Academy of Sciences, Changchun 130033, China
[2]China University of Chinese Academy of Sciences, Beijing 100049, China
*Corresponding author: 18343096308@163.com

Received 31 August 2017; revised 15 October 2017; accepted 15 October 2017; posted 16 October 2017 (Doc. ID 306147); published 13 November 2017

Angle errors of high-order retarders will decrease the accuracy of a channeled spectropolarimeter. This paper presents an easily implemented and widely applicable method for reducing the effects of the angle errors. First, we theoretically derive a modified reconstruction model to express and analyze the effects of the angle errors. Based on the modified reconstruction model and current reference beam calibration technique, we put forward the modified reference beam calibration technique to reduce the effects of the angle errors. This method can calculate the angle errors by employing the amplitude terms, which have been ignored in the results of the current reference beam calibration. The effectiveness of the presented method is verified by numerical simulations, which show that the demodulated deviations of polarization parameters have been reduced by one order of magnitude. Experiments are further implemented to validate the proposed method. The convenience and wide applicability of the presented method make it suitable for regular correction of the instrument, especially for the case on track.

OCIS codes: (120.5410) Polarimetry; (120.6200) Spectrometers and spectroscopic instrumentation; (220.1000) Aberration compensation; (220.1140) Alignment.

https://doi.org/10.1364/AO.56.009156

1. INTRODUCTION

Spectropolarimetry can measure the polarization parameters and spectral content of a light, which has been widely applied in various application fields, such as remote sensing [1–4], material characterization [5,6], and astrophysical study [7]. Several methods for polarization and spectrum acquisition have been put forward [8–10]. Polarimetric spectral intensity modulation (PSIM), which was simultaneously proposed by Iannarilli *et al.* and Oka and Kato in 1999, is one of the most promising methods among them [11,12]. Compared to traditional polarization and spectrum acquisition methods, it has several important advantages, such as the simplicity of the optical system, no mechanically movable components for polarization control or active devices for polarization modulation, and simultaneous measurement of the spectrum and all Stokes parameters in snapshot mode [12]. Since its inception, it has become a popular approach for polarization and spectrum measurement. In recent publications, researchers have investigated combining the PSIM module with other spectrometers [13–17], demodulating spectral content to reconstruct polarization parameters [1,18] and instrument calibration techniques [2,19–23].

In spite of the advantages, application of the PSIM module also poses some problems. Specifically, as will be shown in Section 4 of this paper, when the orientation errors of the fast axes of two high-order retarders are merely 0.5 deg, they can introduce more than 0.008 uncertainty in degree of polarization (DoP) measurement. It obviously exceeds the tolerance in high-accuracy applications [24–26], e.g., the aerosol polarimeter sensor (APS), in which the specification of uncertainty of DoP measurement is less than 0.005 [24]. Oka *et al.* concisely mention and explain the effects of alignment angle errors of retarders [27]. In order to solve the problem, Mu *et al.* use two linearly polarized reference beams oriented at 22.5° and 45° to calculate the orientation errors of two retarders [22]. While its effectiveness has been verified by simulations (without actual experiments), this means has a critical drawback in that it works only when the orientation errors of two retarders are in different signs, which restricts its application. Yang *et al.* propose a calibration method to determine the alignment errors and develop a correction algorithm to compensate them [23]. While the alignment errors of retarders and polarizer can be compensated effectively, we must utilize an additional high-order retarder to determine the errors before the compensation process. Furthermore, the additional high-order retarder must be removed before the instrument works. The placement and removal of the additional high-order retarder increase the

Corrected 29 January 2018

complexity of the system and make it merely suitable for calibration in a laboratory (not suitable for in-orbit application).

To overcome the defects in current methods, this paper presents an easily implemented method to reduce the effects of the angle errors on the precision of a channeled spectropolarimeter. It is applicable for all situations of the angle errors without any additional elements. First, we deduce a modified reconstruction model without any additional elements using Mueller matrices in the presence of the angle errors. The modified reconstruction model clearly shows the effects of the angle errors on each desired channel. Then, based on the modified reconstruction model, we utilize the amplitude terms that have been ignored in the results of the current reference beam calibration to calculate the angle errors. Owing to that the angle errors contained in the amplitude terms are concise to calculate, this method is effective for all situations of the angle errors. According to the modified reconstruction model and calculated results of the angle errors, an easily implemented method for reducing the effects of the angle errors is further proposed. The effectiveness of the proposed method is verified by numerical simulations. The results show that by utilizing the presented method, the measurement accuracy of polarization parameters can be improved by one order of magnitude. Finally, the validity of this method is further verified by experiments.

This paper is structured as follows. Section 2 illustrates the problem of the current demodulation method in the presence of the angle errors. Section 3 theoretically derives the modified reconstruction model and provides a modified demodulation method for reducing the effects of the angle errors. Section 4 verifies the proposed method by numerical simulations. Section 5 validates the proposed method by experimental tests, and conclusions are presented in Section 6.

2. PROBLEM OF THE THEORETICAL DEMODULATION METHOD IN THE PRESENCE OF THE ANGLE ERRORS

In this section, we briefly review the theoretical polarization measurement process of a channeled spectropolarimeter. Based on the theoretical reconstruction model, we simulate the measurement process in the presence of different ranges of the angle errors. Simulation results show that the angle errors apparently decrease the accuracy of polarization measurement.

A. Theoretical Measurement Process of a Channeled Spectropolarimeter

Channeled spectropolarimetry is a technique that converses a spectrometer into a spectropolarimeter through the simple addition of the PSIM module to the optical system. The optical schematic of a spectrometer and PSIM module is shown in Fig. 1. The PSIM module consists of two high-order retarders, R_1 and R_2, with thicknesses d_1 and d_2, respectively, and the polarizer, A.

In this paper, all angles mentioned are in reference to the transmission axis of polarizer A, illustrated in Fig. 1. In theory, as shown in Fig. 1, the transmission axis of polarizer A is horizontal and the fast axes of R_1 and R_2 are 0° and 45°, respectively. In fact, however, due to the alignment errors, the orientation errors of the fast axes of R_1 and R_2 are unavoidable.

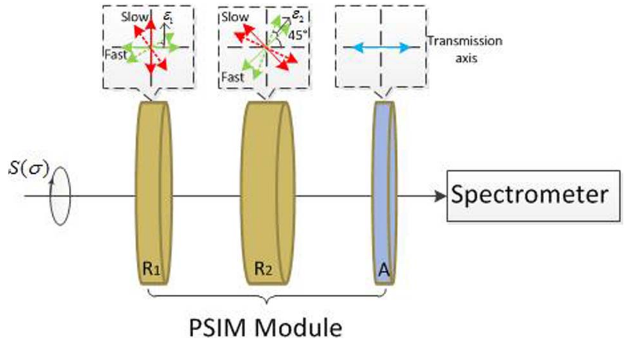

Fig. 1. Sketch of a channeled spectropolarimeter and the angle errors of R_1 and R_2.

ε_1 and ε_2 are the angle errors of R_1 and R_2, respectively, as depicted in Fig. 1.

1. Principle of the Modulation of Spectrally Resolved Stokes Parameters

The polarization parameters of a light passing through a channeled spectropolarimeter can be most conveniently represented in terms of the Stokes vector representation $S = [S_0 S_1 S_2 S_3]^T$. The Stokes vector of a target light launched into the spectrometer is expressed as

$$S_{\text{out}}(\sigma) = M_A(0°) \cdot M_{R_2}\{45°, \varphi_2(\sigma)\} \cdot M_{R_1}\{0°, \varphi_1(\sigma)\} \cdot S_{\text{in}}(\sigma), \tag{1}$$

where $S_{\text{in}}(\sigma)$ and $S_{\text{out}}(\sigma)$ donate the Stokes vectors of incident and transmitted target light, respectively, and σ is the wavenumber. M_{R_1}, M_{R_2}, and M_A stand for the Mueller matrices of R_1, R_2, and A, respectively. $\varphi_j(\sigma)(j = 1, 2)$ is the phase retardation of R_1 and R_2. The spectrum obtained by the spectrometer is expressed as follows [12]:

$$B(\sigma) = \frac{1}{2}S_0(\sigma) + \frac{1}{2}S_1(\sigma)\cos\{\varphi_2(\sigma)\} - \frac{1}{4}|S_{23}(\sigma)|\cos\{\varphi_2(\sigma) + \varphi_1(\sigma) - \arg[S_{23}(\sigma)]\} + \frac{1}{4}|S_{23}(\sigma)|\cos\{\varphi_2(\sigma) - \varphi_1(\sigma) + \arg[S_{23}(\sigma)]\}, \tag{2}$$

where $S_{23}(\sigma) = S_2(\sigma) + iS_3(\sigma)$. $S_k(\sigma)(k = 0\ldots3)$ denotes the Stokes parameters contained in $S_{\text{in}}(\sigma)$, and arg means the operator to take the argument. Computing the autocorrelation function of $B(\sigma)$ with the inverse Fourier transformation, Stokes parameters are modulated to several different frequency domain regions, which are called "channels". The channels distributing in frequency domain are given by

$$C(h) = C_0(h) + C_1[h - (L_1 - L_2)] + C_1^*[-h - (L_1 - L_2)] + C_2(h - L_2) + C_2^*(-h - L_2) + C_3[h - (L_1 + L_2)] + C_3^*[-h - (L_1 + L_2)], \tag{3}$$

where

$$C_0(h) = \mathcal{F}^{-1}\left\{\frac{1}{2}S_0(\sigma)\right\}, \tag{4}$$

$$C_2(h) = \mathcal{F}^{-1}\left\{\frac{1}{4}S_1(\sigma)\exp[i\varphi_2(\sigma)]\right\}, \tag{5}$$

$$C_3(h) = \mathcal{F}^{-1}\left\{-\frac{1}{8}S_{23}(\sigma)\exp[i(\varphi_1(\sigma)+\varphi_2(\sigma))]\right\}, \tag{6}$$

and h is the variable in the frequency domain conjugate to σ under the Fourier transformation. $L_p(p=1,2)$ stands for the actual optical path difference (OPD) introduced by R_1 and R_2 in the central wavenumber [16]. The desired channels, C_0, C_2, and C_3, centered at $h=0$, $h=L_2$, and $h=L_1+L_2$, respectively, are then filtered out by the frequency filtering technique independently, and Fourier transformations are then performed. The results are expressed as

$$\mathcal{F}\{C_0(h)\} = \frac{1}{2}S_0(\sigma), \tag{7}$$

$$\mathcal{F}\{C_2(h)\} = \frac{1}{4}S_1(\sigma)\exp[i\varphi_2(\sigma)], \tag{8}$$

$$\mathcal{F}\{C_3(h)\} = -\frac{1}{8}S_{23}(\sigma)\exp[i(\varphi_1(\sigma)+\varphi_2(\sigma))]. \tag{9}$$

2. *Current Reference Beam Calibration Technique*

As mentioned before, $\varphi_1(\sigma)$ and $\varphi_2(\sigma)$ are the phase retardations of R_1 and R_2, respectively, which are merely the functions of parameters of retarders and wavenumber. To calibrate the phase factors, $\exp[i\varphi_2(\sigma)]$ and $\exp[i(\varphi_1(\sigma)+\varphi_2(\sigma))]$, a reference beam linearly polarized oriented at 22.5° is employed [20,21]. Stokes parameters of the reference beam passing through the PSIM module, are given by

$$S_1(\sigma) = \frac{\sqrt{2}}{2}S_0(\sigma), \tag{10}$$

$$S_2(\sigma) = \frac{\sqrt{2}}{2}S_0(\sigma), \tag{11}$$

$$S_3(\sigma) = 0. \tag{12}$$

Combining Eqs. (4)–(6) and Eqs. (10)–(12), the phase factors are given by

$$\exp[i\varphi_2(\sigma)] = 2\sqrt{2}\frac{\mathcal{F}\{C_{2,22.5^\circ}(h)\}}{\mathcal{F}\{C_{0,22.5^\circ}(h)\}}, \tag{13}$$

$$\exp[i(\varphi_1(\sigma)+\varphi_2(\sigma))] = -4\sqrt{2}\frac{\mathcal{F}\{C_{3,22.5^\circ}(h)\}}{\mathcal{F}\{C_{0,22.5^\circ}(h)\}}. \tag{14}$$

After eliminating the phase factors, the whole Stokes parameters of the incident target light have been acquired as

$$S_0(\sigma) = 2|\mathcal{F}\{C_0(h)\}|, \tag{15}$$

$$S_1(\sigma) = \left|\sqrt{2}\frac{\mathcal{F}\{C_2(h)\}\cdot\mathcal{F}\{C_{0,22.5^\circ}(h)\}}{\mathcal{F}\{C_{2,22.5^\circ}(h)\}}\right|, \tag{16}$$

$$S_2(\sigma) = \mathrm{Re}\left[\frac{\sqrt{2}}{2}\frac{\mathcal{F}\{C_3(h)\}\cdot\mathcal{F}\{C_{0,22.5^\circ}(h)\}}{\mathcal{F}\{C_{3,22.5^\circ}(h)\}}\right], \tag{17}$$

$$S_3(\sigma) = \mathrm{Im}\left[\frac{\sqrt{2}}{2}\frac{\mathcal{F}\{C_3(h)\}\cdot\mathcal{F}\{C_{0,22.5^\circ}(h)\}}{\mathcal{F}\{C_{3,22.5^\circ}(h)\}}\right], \tag{18}$$

where Re is the operator to extract the real part, and Im is the operator to extract the imaginary part.

B. Influences of the Angle Errors on the Accuracy of Degree of Polarization Measurement

It is important to note that the above theoretical polarization measurement process is suitable only for the case in which the PSIM module elements are fixed in their ideal positions. If the orientations of the fast axes of R_1 and R_2 deviate from the ideal state, the angle errors will decrease the accuracy of polarization measurement when this theoretical reconstruction model is utilized.

We utilize Monte Carlo simulations with the above theoretical reconstruction model to calculate the uncertainty of DoP measurement in the presence of various angle errors. During the simulation process, the amplitude ranges of the angle errors are 0°, 0.1°, …, 0.8°. For each specific range, 1000 angle errors are generated randomly, satisfying the uniform distribution from the negative value to the positive value. The 1000 groups of synthetic angle errors for simulations are produced by combining 1000 angle errors of R_1 with 1000 angle errors of R_2, correspondingly. Standard deviations of the simulation results multiplied by the confidence coefficient, whose value is $\sqrt{3}$ for the uniform distribution, are regarded as the final results. The target light for simulations consists of a linearly polarized light oriented at 30° and the natural light (it does not exist when DoP = 1). Owing to that the S_3 parameter stands for the circular polarization, it does not need to measure in remote sensing. Thus, DoP is actually the degree of linear polarization (DoLP), which is calculated using the first three parameters in the Stokes vector [24]. Simulation results obtained from 1000 Monte Carlo trials in the presence of different amplitude ranges of the angle errors are shown in Fig. 2.

As shown in Fig. 2, the uncertainty of DoP measurement grows larger as the angle errors of R_1 and R_2 increase. Besides, the sensitivity of the measurement results to the angle errors also increases with the increase of DoP. Those influences of

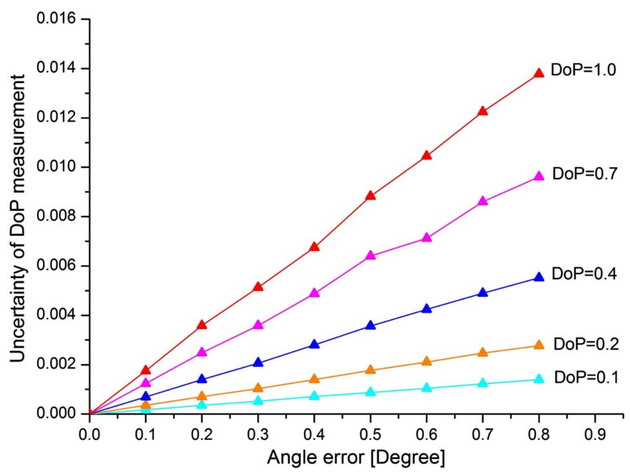

Fig. 2. Uncertainty of DoP measurement in the presence of different angle errors using the theoretical reconstruction model.

Table 1. Requirements of the Angle Error Under Different Situations of Error Assignment

Assigned Uncertainty of DoP	Angle Error Requirement
0.001 (20%)	<0.07 deg
0.002 (40%)	<0.12 deg
0.003 (60%)	<0.17 deg
0.004 (80%)	<0.22 deg
0.005 (100%)	<0.27 deg

the angle errors on the accuracy of polarization measurement cannot be ignored during the assembly and application of a channeled spectropolarimeter. To satisfy the requirements of actual applications, the designed goal of uncertainty of DoP measurement is 0.002–0.005, which varies with the DoP of a target light [24–26]. Besides, the specification is the total uncertainty of DoP, which means that the acceptable uncertainty of DoP measurement introduced by the angle errors is much smaller. Table 1 has listed the requirements of angle errors under different assigned uncertainties of DoP measurement. When the degree of polarization of a target light is DoP = 1, the sensitivity of the accuracy of measurement to the angle errors is the largest. Therefore, the requirements of the angle errors are put forward depending on the 'DoP = 1.0' line in Fig. 2.

As shown in Fig. 2 and Table 1, the requirements of the angle errors are relatively small. In addition, the deviations between the actual and nominal orientations of the fast axes of two high-order retarders are inevitable during the fabrication. Therefore, it is not encouraged to use fine mechanical adjustments during the assembly and application to keep the accuracy of the instrument.

To overcome the inherent limitations of the two methods mentioned in the previous section, we propose a new method using an arbitrary reference beam whose Stokes vector is known to calculate the angle errors. Given that the reference beam calibration technique uses a linearly polarized light oriented at 22.5° to calibrate the phase factors, we modify the reference beam calibration technique for simultaneous acquirement of the angle errors and the phase factors. Compared with the two methods mentioned above, the proposed method is applicative for all situations in the presence of the angle errors. Furthermore, it is easy to implement without any other additional elements. Using the presented method to reconstruct polarization parameters can loosen the demand for the calibration accuracy of the PSIM module while keeping the precision of the instrument. Furthermore, considering the advantages of not needing an additional retarder and being applicable for all situations of the angle errors, the presented method is effective for regular correction of the channeled spectropolarimeter and thus maintains the precision of the instrument in orbit.

3. METHOD FOR REDUCING THE EFFECTS OF THE ANGLE ERRORS

In this section, we derive the modified reconstruction model of the channeled spectropolarimeter, which takes the angle errors of the fast axes of R_1 and R_2 into consideration. Based on the modified reconstruction model, we modify the current reference beam calibration technique and put forward a method to acquire the phase factors and calculate the angle errors simultaneously.

A. Derivation of Modified Reconstruction Model

We first calculate the Stokes vector of the transmitted light, which is expressed as

$$S'_{\text{out}}(\sigma) = M_A(0°) \cdot M_{R_2}\{45° + \varepsilon_2, \varphi_2(\sigma)\} \cdot M_{R_1}\{\varepsilon_1, \varphi_1(\sigma)\} \cdot S_{\text{in}}(\sigma), \tag{19}$$

where $S'_{\text{out}}(\sigma)$ donates the Stokes vector of the transmitted target light in the presence of the angle errors. To explain the derivation process clearly and precisely, we let δ_q substitute for $\varphi_q(\sigma)(q = 1, 2)$ and $\alpha_1 = 0° + \varepsilon_1$ and $\alpha_2 = 45° + \varepsilon_2$ stand for the actual angles of fast axes of R_1 and R_2, respectively. Therefore, the spectrum detected by the spectrometer is expressed as

$$B'(\sigma) = \frac{1}{2}\{K_0 S_0(\sigma) + K_1 S_1(\sigma) + K_2 S_2(\sigma) + K_3 S_3(\sigma)\}, \tag{20}$$

where

$$K_0 = 1, \tag{21}$$

$$\begin{aligned} K_1 = {} & b^2c^2 \cdot \cos(\delta_1) - ac \cdot \sin(\delta_1) \cdot \sin(\delta_2) \\ & + b^2d^2 + a^2c^2 \cdot \cos(\delta_1) \\ & + abcd \cdot \{1 - \cos(\delta_1)\} \cdot \{1 - \cos(\delta_2)\} \\ & + a^2d^2 \cdot \cos(\delta_1), \end{aligned} \tag{22}$$

$$\begin{aligned} K_2 = {} & bc \cdot \sin(\delta_1) \cdot \sin(\delta_2) \\ & + abc^2 \cdot \{1 - \cos(\delta_1)\} \cdot \cos(\delta_2) \\ & + b^2cd \cdot \cos(\delta_1) \cdot \{1 - \cos(\delta_2)\} \\ & + abd^2 \cdot \{1 - \cos(\delta_1)\} + a^2cd \cdot \{1 - \cos(\delta_2)\}, \end{aligned} \tag{23}$$

$$\begin{aligned} K_3 = {} & -c \cdot \cos(\delta_1) \cdot \sin(\delta_2) \\ & + bcd \cdot \sin(\delta_1) \cdot \{1 - \cos(\delta_2)\} \\ & - ac^2 \cdot \sin(\delta_1) \cdot \cos(\delta_2) - ad^2 \cdot \sin(\delta_1). \end{aligned} \tag{24}$$

In Eqs. (22)–(24), $a = \sin(2\alpha_1)$, $b = \cos(2\alpha_1)$, $c = \sin(2\alpha_2)$, and $d = \cos(2\alpha_2)$. Because the angle errors of fast axes of retarders are relatively small, small-angle approximations have been applied to simplify the coefficients $K_r(r = 1, 2, 3)$. a and d are first-order small quantities. a^2, d^2, and ad are second-order small quantities. By ignoring the second-order and higher-order small quantities and performing proper trigonometric function transformations, we can deduce the expression of $B'(\sigma)$, which is given by

$$\begin{aligned} B'(\sigma) = {} & \frac{1}{2}S_0(\sigma) + \frac{1}{2}S_1(\sigma)\cos\{\varphi_2(\sigma)\} + \Delta_1 \\ & - \frac{1}{4}|S_{23}(\sigma)|\cos\{\varphi_2(\sigma) + \varphi_1(\sigma) - \arg[S_{23}(\sigma)]\} + \Delta_2 \\ & + \frac{1}{4}|S_{23}(\sigma)|\cos\{\varphi_2(\sigma) - \varphi_1(\sigma) + \arg[S_{23}(\sigma)]\} + \Delta_3 + \Delta_4, \end{aligned} \tag{25}$$

where

$$\Delta_1 = \varepsilon_1 S_2(\sigma)\cos\{\varphi_2(\sigma)\}, \quad (26)$$

$$\Delta_2 = -\frac{1}{2}(\varepsilon_1 - \varepsilon_2)|S_{23}(\sigma)|\cos\{\varphi_2(\sigma) + \varphi_1(\sigma) - \arg[S_{23}(\sigma)]\} + \frac{1}{2}\varepsilon_1 S_1(\sigma)\cos\{\varphi_2(\sigma) + \varphi_1(\sigma)\}, \quad (27)$$

$$\Delta_3 = -\frac{1}{2}(\varepsilon_1 - \varepsilon_2)|S_{23}(\sigma)|\cos\{\varphi_2(\sigma) - \varphi_1(\sigma) + \arg[S_{23}(\sigma)]\} - \frac{1}{2}\varepsilon_1 S_1(\sigma)\cos\{\varphi_2(\sigma) - \varphi_1(\sigma)\}, \quad (28)$$

$$\Delta_4 = -\varepsilon_1 |S_{23}(\sigma)|\cos\{\varphi_1(\sigma) - \arg[S_{23}(\sigma)]\}. \quad (29)$$

Computing the autocorrelation function of $B'(\sigma)$ with the inverse Fourier transformation, the result is expressed as

$$C'(h) = C_0'(h) + C_1'[h - (L_1 - L_2)] + C_1'^*[-h - (L_1 - L_2)] + C_2'(h - L_2) + C_2'^*(-h - L_2) + C_3'[h - (L_1 + L_2)] + C_3'^*[-h - (L_1 + L_2)] + C_4'(h - L_1) + C_4'^*(-h - L_1), \quad (30)$$

where

$$C_0'(h) = \mathcal{F}^{-1}\left\{\frac{1}{2}S_0(\sigma)\right\}, \quad (31)$$

$$C_2'(h) = \mathcal{F}^{-1}\left\{\left\{\frac{1}{4}S_1(\sigma) + \frac{1}{2}\varepsilon_1 S_2(\sigma)\right\}\exp[i\varphi_2(\sigma)]\right\}, \quad (32)$$

$$C_3'(h) = \mathcal{F}^{-1}\left\{\begin{array}{l} -\left(\frac{1}{8} + \frac{1}{4}(\varepsilon_1 - \varepsilon_2)\right)S_{23}^*(\sigma)\exp[i(\varphi_1(\sigma) + \varphi_2(\sigma))] \\ +\frac{1}{4}\varepsilon_1 S_1(\sigma)\exp[i(\varphi_1(\sigma) + \varphi_2(\sigma))] \end{array}\right\}, \quad (33)$$

where $S_{23}^*(\sigma) = S_2(\sigma) - iS_3(\sigma)$. Comparing Eqs. (4)–(6) with Eqs. (31)–(33), the reconstruction model has been changed by the angle errors apparently. The Stokes parameters reconstructed from the desired channels $C_2'(h)$ and $C_3'(h)$ are not the true values because of the effects of the angle errors. Comparing Eq. (3) and with Eq. (30), new channels $C_4'(h)$ and $C_4'^*(h)$ have been created when ε_2 exists. However, they could not be utilized for error determination owing to their practically overlapping with channels $C_1'(h)$ and $C_1'^*(h)$, respectively, which is caused by the thickness ratio of R_1 and R_2 being 1:2.

Because the angle errors are relatively small, fine mechanical adjustments will cost plenty of expense. Furthermore, it is inconvenient to adjust when the channeled spectropolarimeter is in orbit. Based on the results of derivation, we modify the current reference beam calibration technique and propose a demodulation method to reduce the effects of the angle errors of the fast axes of R_1 and R_2.

B. Modified Reference Beam Calibration Technique

The current reference beam calibration technique is able to acquire two complex coefficients, which contain two amplitude terms and two phase terms. Phase terms are generally used to calibrate the phase factors, while amplitude terms are ignored, usually. According to the modified reconstruction model derived in the previous part of this section, we modify the current reference beam calibration technique in which we calculate the orientation errors using amplitude terms and calibrate the phase factors using phase terms simultaneously.

When the reference-beam linearly polarized light oriented at 22.5° passes through the PSIM module, combining Eqs. (10)–(12) and Eqs. (31)–(33), the demodulation results are given by

$$\frac{\mathcal{F}\{C'_{2,22.5^\circ}(h)\}}{\mathcal{F}\{C'_{0,22.5^\circ}(h)\}} = \frac{\sqrt{2}}{4}(1 + 2\varepsilon_1)\exp[i\varphi_2(\sigma)], \quad (34)$$

$$\frac{\mathcal{F}\{C'_{3,22.5^\circ}(h)\}}{\mathcal{F}\{C'_{0,22.5^\circ}(h)\}} = -\frac{\sqrt{2}}{8}(1 - 2\varepsilon_2)\exp[i(\varphi_1(\sigma) + \varphi_2(\sigma))]. \quad (35)$$

The angle errors ε_1 and ε_2 can be calculated by extracting the amplitude terms, given by

$$\varepsilon_1 = \frac{2\sqrt{2}\left|\frac{\mathcal{F}\{C'_{2,22.5^\circ}(h)\}}{\mathcal{F}\{C'_{0,22.5^\circ}(h)\}}\right| - 1}{2}, \quad (36)$$

$$\varepsilon_2 = \frac{-4\sqrt{2}\left|\frac{\mathcal{F}\{C'_{3,22.5^\circ}(h)\}}{\mathcal{F}\{C'_{0,22.5^\circ}(h)\}}\right| + 1}{2}. \quad (37)$$

The actual phase retardations $\varphi_1(\sigma)$ and $\varphi_2(\sigma)$ are calibrated by extracting the phase terms as usual. Since the actual phase factors and the angle errors contained in the modified reconstruction model are settled, combining Eqs. (31)–(37), the Stokes vector of the target light can be figured out to discover the true polarization contents.

It is shown that the angle errors contained in amplitude terms expressed in Eqs. (36) and (37) are really concise to calculate. It makes this method applicable to determining all kinds of angle errors without any additional devices.

4. VERIFICATION BY NUMERICAL SIMULATIONS

The effectiveness of this presented method is first verified by numerical simulations. In the simulations, two linearly polarized lights, the reference beam oriented at 22.5° and the target light oriented at 30°, are employed. The wavenumber range is $11,000$–$15,467\ \mathrm{cm}^{-1}$, and the thicknesses of R_1 and R_2 are 3.5 mm and 7.0 mm, respectively. The high-order retarders are made of quartz, whose birefringence in the selected waveband can be consulted in Ref. [9]. The comparison of reconstructed polarization parameters using two methods, i.e., traditional method [20,21] and presented method here, are presented in this section.

To describe the typical effects of the angle errors on the modulated spectrum, we provide the magnitude of the autocorrelation function of the obtained spectrum under the situation of $\varepsilon_1 = \varepsilon_2 = 0.5°$. The simulation results are presented in Fig. 3.

Figure 3 shows that the seven channels included in $C(h)$ are satisfactorily separated from one another over the h axis, owing to that the thicknesses of the retarders are selected properly.

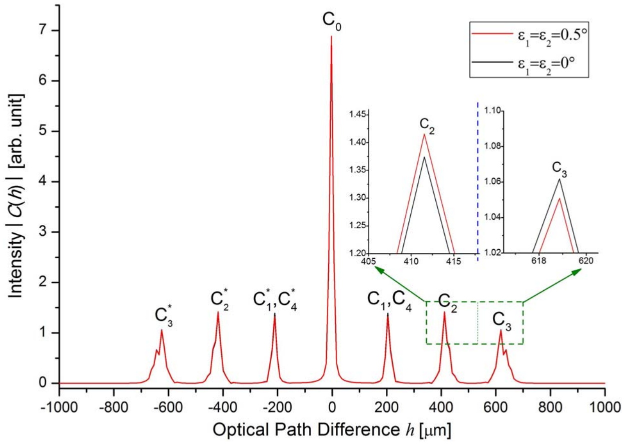

Fig. 3. Magnitude of the autocorrelation function of the modulated spectrum. The enlarged part in the dashed box shows the typical difference.

Comparing two curves in Fig. 3, all channels are almost overlapped and centered at the same location in the h axis, which means the angle errors of the fast axes of R_1 and R_2 do not affect their phase retardations, which agrees with the theoretical derivation [28]. C_1 and C_4 are overlapped because the thickness ratio of R_1 and R_2 is selected as 1:2, which is consistent with the modified reconstructed model in Eq. (30). These results further suggest that we cannot use channels C_1 and C_4 to reconstruct the Stokes parameters or calculate the angle errors.

The typical effects of the angle errors are similar, which just grow larger with the increase of the angle errors. Based on the modified reconstruction model, we can utilize the presented method to reduce the effects of the angle errors and acquire the true polarization parameters. The comparison of reconstructed uncertainty of DoP using two methods obtained from 1000 Monte Carlo trials are presented in Fig. 4 (the process of Monte Carlo simulations is introduced in Subsection 2.B).

Figure 4 clearly shows that the presented method has effectively reduced the effects of the angle errors. The results indicate that we can relax the alignment tolerances of the PSIM module elements in ground-based assembly while keeping the accuracy of the instrument.

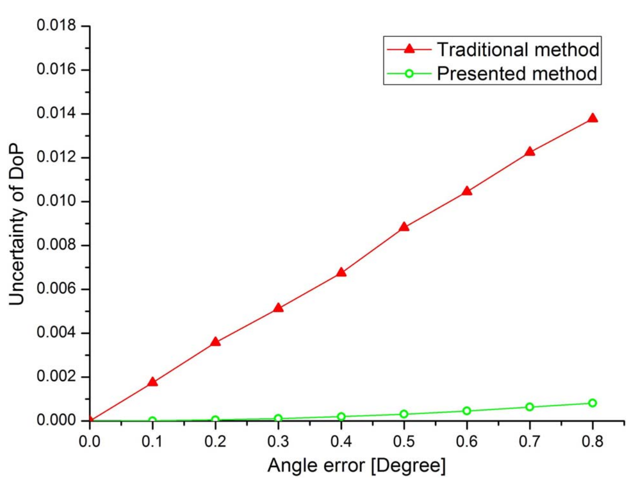

Fig. 4. Uncertainty of DoP in the presence of different angle errors when the input value is DoP = 1.

Then we calculate the polarization parameters utilizing two demodulation methods when the angle errors are in a specific situation of $\varepsilon_1 = \varepsilon_2 = 0.5°$. The calculated results of the angle errors are shown in Fig. 5. The maximum deviation and average deviation of calculated errors are listed in Table 2. Because the angle errors are independent of wavenumber, we can use the averages of the calculated values in different wavenumbers as the final calculation results.

As shown in Table 2, the average errors of the calculated results of ε_1 and ε_2 are −0.0092° and 0.0064°, respectively. These results indicate that we can determine the angle errors accurately using the presented method, which is significant for reconstructing polarization parameters.

The influences of the angle errors and the effectiveness of the presented method are shown in Figs. 6 and 7. Table 3 lists the reconstructed deviations of polarization parameters in the presence of $\varepsilon_1 = \varepsilon_2 = 0.5°$. Comparing the reconstructed results using two different demodulation techniques, the maximum deviations and the average deviations of S_1/S_0, S_2/S_0 and DoP have deduced by one order of magnitude. That is to say, the effects of the angle errors have been reduced effectively. Owing to that the angle errors are $\varepsilon_1 = \varepsilon_2$, two demodulated curves of S_3/S_0 are overlapping. It is consistent with the theoretical derivation, which further illustrates the validity of the modified reconstruction model. Taking into account the overlap of two curves, the results of S_3/S_0 do not need to be listed in Tables 3 and 4, which does not affect the comprehension of the conclusions.

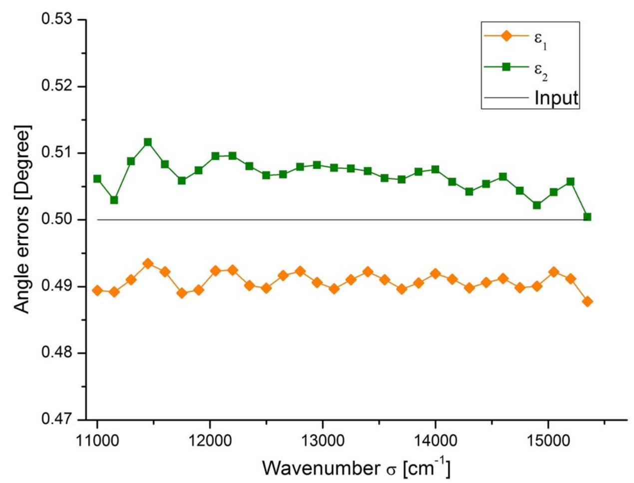

Fig. 5. Calculated results of the angle errors.

Table 2. Comparison of Calculated Results of ε_1 and ε_2

Parameter	Maximum Calculated Error	Average Calculated Error
ε_1	−0.0127°	−0.0092°
ε_2	0.0117°	0.0064°

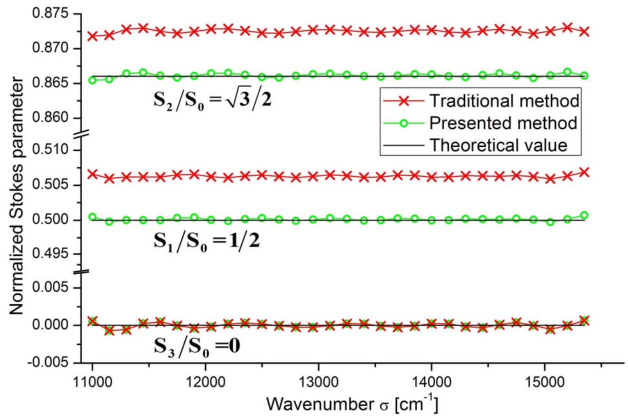

Fig. 6. Reconstructed results of normalized Stokes parameters. The theoretical values are $S_1/S_0 = 1/2$, $S_2/S_0 = \sqrt{3}/2$, and $S_3/S_0 = 0$.

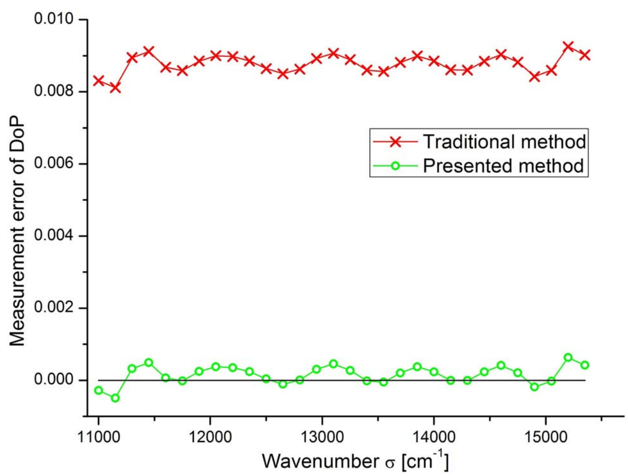

Fig. 7. Reconstructed errors of the DoP.

The above results demonstrate that the influences of the angle errors have been reduced greatly. This method is effective to achieve high precision of the instrument while relaxing the tolerance of assembly errors of the PSIM module. Furthermore, the presented method can work effectively without any additional elements or precise mechanical adjustments. When the instrument works in orbit, using this method for regular correction is effective and convenient to maintain the accuracy of polarization measurement.

Table 3. Comparison of Reconstructed Deviations of Two Methods

Deviation Type	Demodulation Method	S_1/S_0	S_2/S_0	DoP
Maximum deviation	Traditional method	6.88×10^{-3}	7.04×10^{-3}	9.33×10^{-3}
	Presented method	7.23×10^{-4}	-7.08×10^{-4}	7.17×10^{-4}
Average deviation	Traditional method	6.28×10^{-3}	6.49×10^{-3}	8.77×10^{-3}
	Presented method	1.20×10^{-4}	1.11×10^{-4}	1.56×10^{-4}

5. ANALYSIS OF EXPERIMENTAL RESULTS

The validity of the presented method is further verified by experimental tests. The two essential components of the experimental setup are a high-stability broadband light source and a fine-spectral-resolution channeled spectropolarimeter, which are shown in Fig. 8. The light source consists of a stabilized tungsten halogen lamp and a collimator. The channeled spectropolarimeter consists of the PSIM module (the retarders R_1 and R_2 and polarizer A in the dashed box) and a spectrometer (FieldSpec 3, Analytical Spectral Devices). The rotatable polarizer P is used to generate the reference beam oriented at 22.5° and the target light oriented at 30°.

The thicknesses of R_1 and R_2 and the wavenumber range are consistent with the simulation settings. The retarders R_1 and R_2 and polarizers A and P are placed in precision-adjusting racks for satisfying various experimental test conditions.

During the experimental test process, we select four angle error situations, i.e., $\varepsilon_1 = \varepsilon_2 = 0.1°, 0.3°, 0.5°, 0.8°$, to verify the presented method. The initial state after alignment is regarded as the situation $\varepsilon_1 = \varepsilon_2 = 0°$. Then, we artificially introduce the angle errors based on the initial state to simulate the actual situations. Meanwhile, the states of the other experimental setup remain unchanged. In each situation of the angle errors, we measure the modulated spectrum illuminating the system with the target light and the reference beam, respectively.

We provide the magnitude of the autocorrelation function of the measured spectrum in the presence of angle errors $\varepsilon_1 = \varepsilon_2 = 0.5°$, which is shown in Fig. 9. We find that the seven channels are separated from one another over the h axis, which is consistent with the modified reconstruction model and simulation results. It is noteworthy that the positions of channels C_0 and C_1 are consistent with the simulation results. However, the positions of channels C_2 and C_3 are slightly shifted right over the h axis compared with the simulation results, which may be caused by the thickness deviation of the high-order retarder R_2.

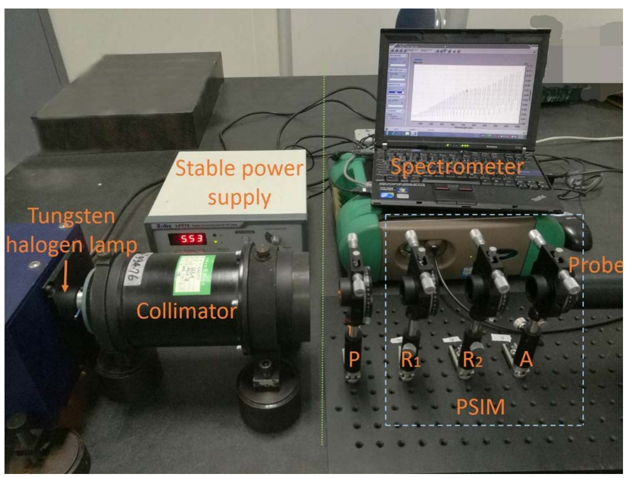

Fig. 8. Photograph of the experimental setup.

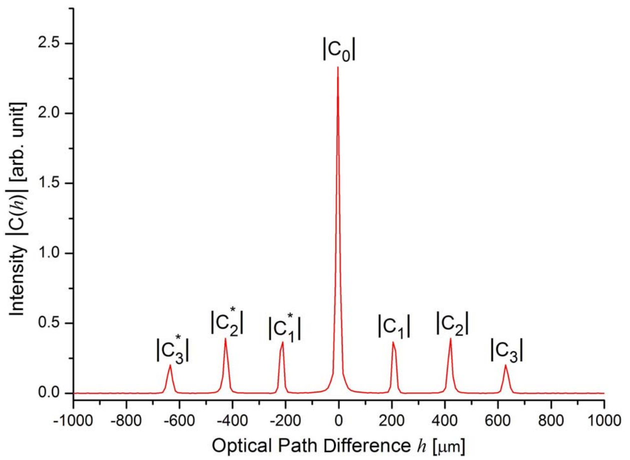

Fig. 9. Autocorrelation function $|C(h)|$ of measured spectrum in the presence of angle errors $\varepsilon_1 = \varepsilon_2 = 0.5°$.

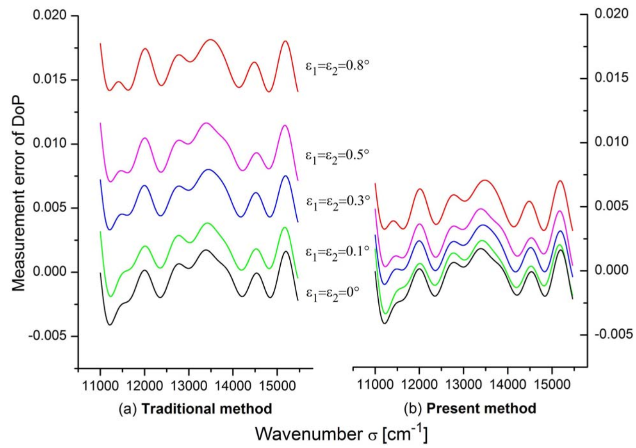

Fig. 11. Reconstructed errors of DoP under different situations of the angle errors.

Based on Eqs. (36) and (37), we can calculate the angle errors of R_1 and R_2 and reduce the demodulation deviations introduced by the angle errors. Figures 10 and 11 show the comparison of polarization parameters reconstructed from measurements in the presence of different angle errors using the presented method and the traditional method. As shown in Figs. 10(a) and 11(a), the results demodulated by the traditional method clearly show that demodulation deviations grow larger as the angle errors increase. Therefore, to keep the accuracy of the measurement, the effects of the angle errors of the retarders cannot be ignored. As shown in Figs. 10(b) and 11(b), using the presented method here, the deviations of demodulated polarization parameters have decreased, which means that the effects of the angle errors have been reduced largely. It is worth noting that the presented method is applicable for all situations of angle errors without any additional elements or mechanical adjustments.

Comparing the reconstructed results using the two different methods in Table 4, the reconstructed deviations have decreased obviously. By using the presented method for reducing the effects of the angle errors, the residual average deviations of S_1/S_0, S_2/S_0, and DoP are 7.22×10^{-4}, 2.58×10^{-3}, and 2.59×10^{-3}, respectively. The accuracy of experimental tests may be affected by the vibration of reconstructed results, although we have alleviated the influences through introducing apodization using the Hann window [29]. As indicated in Eq. (33), owing to that the angle errors are $\varepsilon_1 = \varepsilon_2$, the reconstructed results of S_3 are not influenced by the angle errors. This is the reason for the similarity in the curves of S_3 demodulated by two different methods. Furthermore, because the theoretical value of S_3 is zero, it may be influenced by the noises of the spectrometer, which causes the curves of reconstructed S_3 not to have the regular pattern like other polarization parameters. On the whole, the results above indicate that the presented method is effective to reduce the influences of the angle errors.

The experimental results demonstrate that by using the presented method to reduce the effects of the angle errors, the accuracy of the reconstructed polarization parameters can be improved under different situations of the angle errors. In consideration of the influences of the vibration, stress, or other factors in an application [23], the convenience and wide applicability of the presented method make it suitable to termly calibrate the channeled spectropolarimeter in orbit. It is significant for practical applications of the channeled spectropolarimeter.

Table 4. Comparison of Reconstructed Results Using Two Different Demodulation Methods Under $\varepsilon_1 = \varepsilon_2 = 0.5°$

Deviation Type	Demodulation Method	S_1/S_0	S_2/S_0	DoP
Maximum deviation	Traditional method	6.98×10^{-3}	1.03×10^{-2}	1.16×10^{-2}
	Presented method	2.10×10^{-3}	5.28×10^{-3}	4.84×10^{-3}
Average deviation	Traditional method	5.61×10^{-3}	7.57×10^{-3}	9.36×10^{-3}
	Presented method	7.22×10^{-4}	2.58×10^{-3}	2.59×10^{-3}

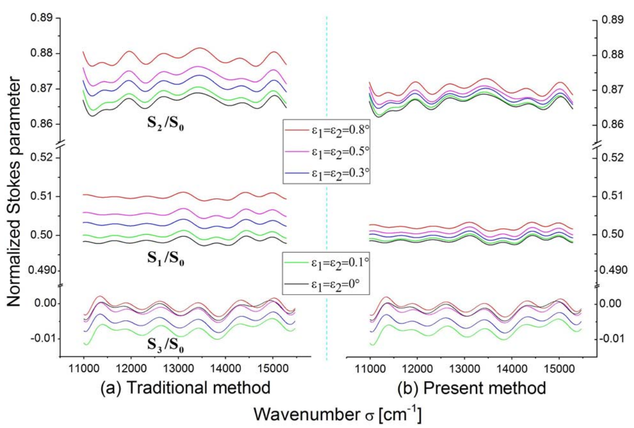

Fig. 10. Reconstructed Stokes parameters using two demodulation methods.

6. CONCLUSIONS

The angle errors decrease the accuracy of the channeled spectropolarimeter apparently. The current methods are either effective only in special situations of the angle errors or complex in calibrating the angle errors. In this paper, we present a widely applicable and easily implemented method for reducing the effects of the angle errors for the instrument. A modified reconstruction model without any additional elements considering the angle errors is theoretically derived. It clearly demonstrates the crosstalk between the desired channels caused by the angle errors. A modified reference beam calibration technique, utilizing the amplitude terms that have been ignored in the current reference beam calibration technique, is proposed to calculate the angle errors. Because the angle errors contained in the amplitude terms are concise to calculate, this method is effective for all situations in the presence of the angle errors. Simulation results show that the maximum deviations and average deviations of demodulated polarization parameters are reduced by one order of magnitude. The effectiveness of the presented method is further verified by experiments.

Compared with current methods, the advantages of being applicable for all situations of the angle errors and not needing additional elements make it more applicable and convenient for use. By employing the presented method, we can relax the alignment tolerances of the PSIM module elements in ground-based assembly of the instrument. Furthermore, we can use the presented method for regular correction for the channeled spectropolarimeter in orbit to reduce the effects of the angle errors. It is effective and convenient to maintain the accuracy of the measurement of polarization parameters, which has an important significance for the application of the channeled spectropolarimeter.

Funding. National Natural Science Foundation of China (NSFC) (61505199); National Key Research and Development Program (2016YFF0103603).

REFERENCES

1. F. Snik, T. Karalidi, and C. U. Keller, "Spectral modulation for full linear polarimetry," Appl. Opt. **48**, 1337–1346 (2009).
2. S. H. Jones, F. J. Iannarilli, and P. L. Kebabian, "Realization of quantitative-grade fieldable snapshot imaging spectropolarimeter," Opt. Express **12**, 6559–6573 (2004).
3. A. D. Noia, O. P. Hasekamp, G. Harten, J. H. H. Rietjens, J. M. Smit, F. Snik, J. S. Henzing, J. Boer, C. U. Keller, and H. Volten, "Use of neural networks in ground-based aerosol retrievals from multi-angle spectropolarimetric observations," Atmos. Meas. Tech. **8**, 281–299 (2015).
4. H. J. Hoeijmakers, M. L. J. Arts, F. Snik, C. U. Keller, D. M. Stam, and J. M. Kuiper, "Design trade-off and proof of concept for LOUPE, the Lunar Observatory for Unresolved Polarimetry of Earth," Opt. Express **24**, 21435–21453 (2016).
5. D. Kim, Y. Seo, Y. Yoon, V. Dembele, J. W. Yoon, K. J. Lee, and R. Magnusson, "Robust snapshot interferometric spectropolarimetry," Opt. Lett. **41**, 2318–2321 (2016).
6. M. Dubreuil, S. Rivet, B. Le Jeune, and L. Dupont, "Time-resolved switching analysis of a ferroelectric liquid crystal by snapshot Mueller matrix polarimetry," Opt. Lett. **35**, 1019–1021 (2010).
7. M. Pertenais, C. Neiner, P. Bernardi, J.-M. Reess, and P. Petit, "Static spectropolarimeter concept adapted to space conditions and wide spectrum constraints," Appl. Opt. **54**, 7377–7386 (2015).
8. B. Henderson, "Spectroscopic measurements," in *Handbook of Optics*, M. Bass, ed. (McGraw-Hill, 1995).
9. R. A. Chipman, "Polarimetry," in *Handbook of Optics*, M. Bass, ed. (McGraw-Hill, 1995).
10. J. S. Tyo, D. L. Goldstein, D. B. Chenault, and J. A. Shaw, "Review of passive imaging polarimetry for remote sensing applications," Appl. Opt. **45**, 5453–5469 (2006).
11. F. J. Iannarilli, S. H. Jones, H. E. Scott, and P. Kebabian, "Polarimetric-Spectral Intensity Modulation (P-SIM): enabling simultaneous hyperspectral and polarimetric imaging," Proc. SPIE **3698**, 474–481 (1999).
12. K. Oka and T. Kato, "Spectroscopic polarimetry with a channeled spectrum," Opt. Lett. **24**, 1475–1477 (1999).
13. A. M. Locke, D. S. Sabatke, E. L. Dereniak, M. R. Descour, J. P. Garcia, T. Hamilton, and R. W. McMillan, "Snapshot imaging spectropolarimeter," Proc. SPIE **4481**, 64–72 (2002).
14. N. Hagen, A. M. Locke, D. S. Sabatke, E. L. Dereniak, and D. T. Sass, "Methods and applications of snapshot spectropolarimetry," Proc. SPIE **5432**, 167–174 (2004).
15. R. W. Aumiller, C. Vandervlugt, E. L. Dereniak, R. Sampson, and R. W. McMillan, "Snapshot imaging spectropolarimetry in the visible and infrared," Proc. SPIE **6972**, 69720D (2008).
16. J. Li, J. Zhu, and H. Wu, "Compact static Fourier transform imaging spectropolarimeter based on channeled polarimetry," Opt. Lett. **35**, 3784–3786 (2010).
17. C. Zhang, Q. Li, T. Yan, T. Mu, and Y. Wei, "High throughput static channeled interference imaging spectropolarimeter based on a Savart polariscope," Opt. Express **24**, 23314–23332 (2016).
18. D. S. Sabatke, A. M. Locke, E. L. Dereniak, and R. W. McMillan, "Linear calibration and reconstruction techniques for channeled spectropolarimetry," Opt. Express **11**, 2940–2952 (2003).
19. N. Hagen, E. L. Dereniak, and D. T. Sass, "Visible snapshot imaging spectro-polarimeter," Proc. SPIE **5888**, 277–286 (2005).
20. A. Taniguchi, H. Okabe, H. Naito, N. Nakatsuka, and K. Oka, *Polarization Science and Remote Sensing II* (SPIE, 2005), p. 588811.
21. A. Taniguchi, K. Oka, H. Okabe, and M. Hayakawa, "Stabilization of a channeled spectropolarimeter by self-calibration," Opt. Lett. **31**, 3279–3281 (2006).
22. T. Mu, C. Zhang, C. Jia, W. Ren, L. Zhang, and Q. Li, "Alignment and retardance errors, and compensation of a channeled spectropolarimeter," Opt. Commun. **294**, 88–95 (2013).
23. B. Yang, X. Ju, C. Yan, and J. Zhang, "Alignment errors calibration for a channeled spectropolarimeter," Opt. Express **24**, 28923–28935 (2016).
24. R. J. Peralta, C. Nardell, B. Cairns, E. E. Russell, L. D. Travis, M. I. Mishchenko, and R. J. Hooker, "Aerosol polarimetry sensor for the Glory Mission," Proc. SPIE **6786**, 67865L (2007).
25. S. Persh, Y. J. Shaham, O. Benami, B. Cairns, M. I. Mishchenko, J. D. Hein, and B. A. Fafaul, "Ground performance measurements of the Glory aerosol polarimetry sensor," Proc. SPIE **7807**, 780703 (2010).
26. D. J. Diner, R. A. Chipman, N. Beaudry, B. Cairns, L. D. Foo, S. A. Macenka, and C. Keller, *Enabling Sensor and Platform Technologies for Spaceborne Remote Sensing* (SPIE, 2004), p. 88.
27. K. Oka, A. Taniguchi, and H. Okabe, "Spectroscopic polarimetry," U.S. patent 7623236 B2 (24 November 2009).
28. J. Dong and Y. Li, "Analysis and optimization approaches for wide-viewing-angle $\lambda/4$ plate in polarimetry for immersion lithography," J. Vac. Sci. Technol. B **31**, 011602 (2013).
29. D. S. Sabatke, "Snapshot spectropolarimetry," Ph.D. dissertion (University of Arizona, 2002).